

Low Frequency Geoacoustic Inversion Method

A. Tolstoy
1538 Hampton Hill Circle, McLean VA 22101
phone: (703) 760-0881 email: atolstoy@ieee.org

Award Number: N00014-10-C-0022

LONG TERM GOALS

The primary long term objective of this project is to:

- determine a *fast and accurate* inversion method to estimate bottom properties in shallow water.

OBJECTIVES

The objectives of this year's work (FY12) included:

- *continued* study of a *new* deterministic low frequency (LF) geoacoustic inversion (G.I.) method recently featuring the minimization processor (Tolstoy, '10 and '12);
- *demonstration* that horizontal arrays can be successfully used for G.I. with the new method (presented at the fall ASA);
- *preparation* the LF G.I. method to be applied to ranges beyond 2 km (KRAKEN was integrated into the processing software in preparation for the D. Knobles data);
- *initiation* of efforts for the consideration of frequencies above 100Hz at close range (leading to consideration of such frequencies at longer ranges; this was suggested by K. Becker this past spring). We have already seen that at ranges beyond 1km and at freqs above 100Hz inversion can be problematic if all geoacoustic, environmental, and geometric parameters are unknown.

APPROACH

The LF method performs an *exhaustive* search through a *finite* parameter space. We have seen previously that some parameters are inextricably paired, e.g., source range *rge* and water depth *D*. Taking account of such relationships can help to reduce the search space, particularly for frequencies below 100Hz. We also note excellent sensitivity for our low frequencies to some geoacoustic parameters such as sediment sound-speed in the underlying half-space c_{hsp} depending on frequency *f* and *rge*.

For the minimization approach proposed here $\mathcal{P}_{min}(\mathbf{p})$ at the vector parameter combination \mathbf{p} we require that for \mathbf{p} in our search space only the minimum processor value (over *f*) be retained. Thus,

all frequencies considered at that point will have processor values at least as great as the final value. Consequently, (1) the frequency most sensitive to a parameter dominates the search automatically, and (2) resolution has improved with major sidelobe reduction. The method is intended primarily for geoacoustic inversion methods (where the signal-to-noise levels are high).

For the simulations we shall continue to consider one single sediment layer scenario (each defined by a linear sound-speed profile and constant density) over a half-space (constant sound-speed and density) each at multiple frequencies (25 to 100Hz, although recent efforts have begun investigations for 100 to 200 Hz) and multiple ranges (250m to 2km while recent efforts have considered ranges up to 5km).

The “true” environments for these simulations (based on SW06 test scenarios) are shown in Fig.1 and Table 1 allowing for thin, medium, and thick sediment layers. Consideration of a variety of scenarios helps to address concerns that our conclusions, particularly with regard to frequency, are very dependent on sediment thickness. For the “exact” inversion processing to be discussed below we shall assume that:

- the bottom consists of a single linear sediment layer (specified by c_{top} , γ , and h_{sed} , over a half-space with sound-speed c_{hsp}) (parameters will vary depending on the layer thickness under consideration; see Table 1);
- all water depths D will be within 78 to 86m (parameter value will vary depending on the layer thickness under consideration; see Table 1);
- the fixed source ranges rge will each be less than about 2km;
- the ocean sound-speed $c(z)$ will vary with depth only (no inversion on $c(z)$; see the solid curve in Fig. 1);
- z_{sou} will be fixed (no inversion done on z_{sou});
- we have only one array which will be vertical (VLA) with length 56.25m consisting of 16 phones spaced at 3.75m apart with array element localization and top phone depth at $z_{ph1} = 14.6m$ or $z_{ph1} = 15.6m$. Alternately, we have also considered horizontal arrays (HLAs) with various lengths and a variety of phones numbers, depths z_{ph} , and spacings. The “true” arrays have no tilt.

As in the earlier simulation work, we will generate the “true” field using the single depth-variable ocean sound-speed profile seen as the solid curve of Fig. 1 (top), and as before we shall continue to generate the synthetic acoustic fields via RAMGEO (Collins, '94).

Broadband (BB) frequency averaging for the improvement of matched field processing (MFP) has been around for over twenty years, particularly for the suppression of sidelobes (Tolstoy, '93). For each f the MFP values at sidelobes (non-true parameter values) can vary quite a bit. Simple incoherent summation $\mathcal{P}_{lin,ave}(\mathbf{p})$ (see Tolstoy, '12b) can be quite stable with values following the high level MFP values while not diminishing much for an occasional low MFP value. Such an approach (with the linear processor) is often used for data plus a Bayesian inversion to estimate geoacoustic parameters (Chapman & Jiang, '08). Incoherent linear summation is also an ingredient in many inversions using genetic algorithms (Gerstoft et al., '03).

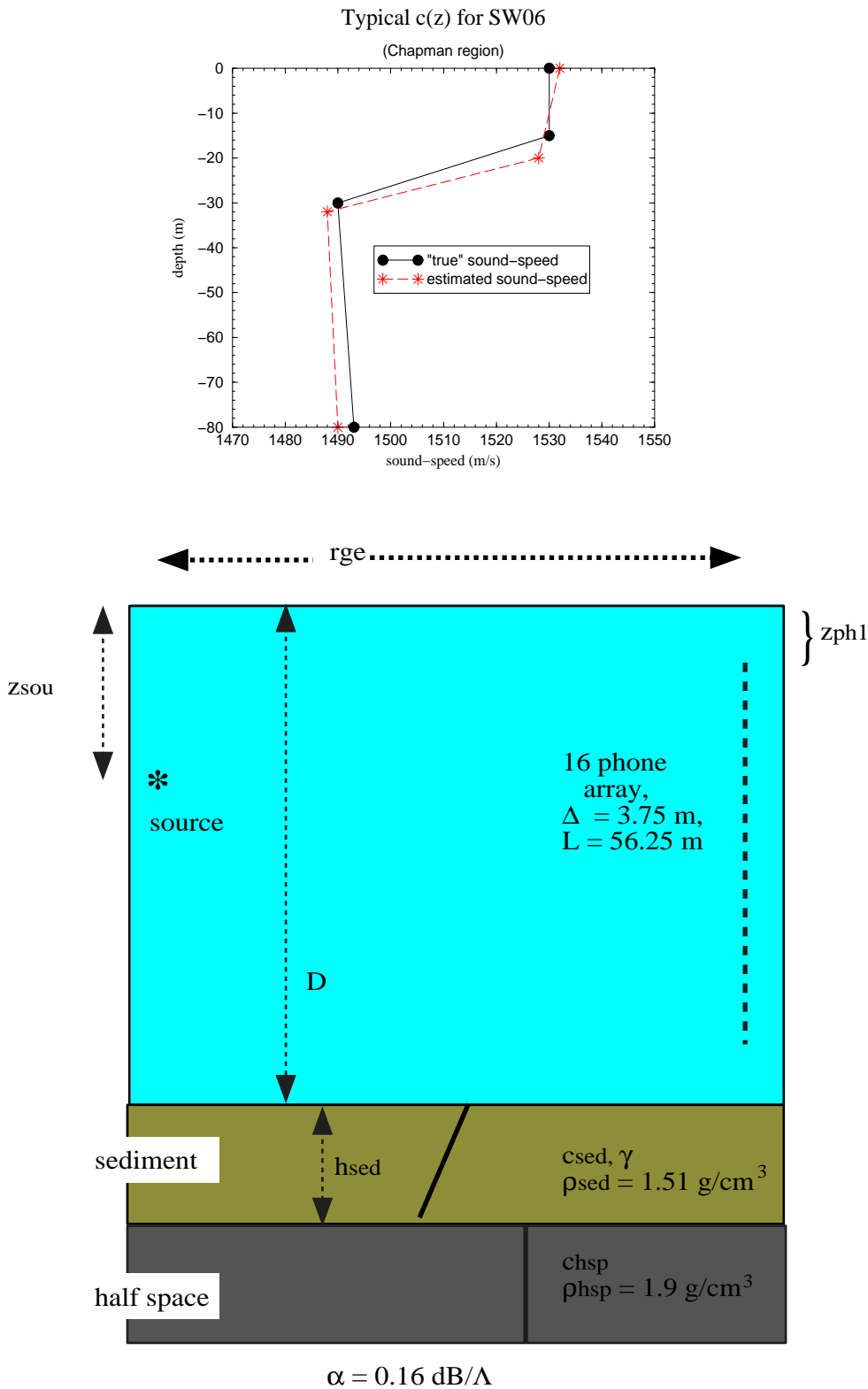


Figure 1: Plot of simulated SW06 environment where the upper subplot shows the ocean sound-speed $c(z)$ used in the simulations (the exact and approximate profiles shown), and the lower subplot shows the ocean waveguide assuming the linear sound-speed profile in a single sediment layer over a half-space basement. Actual bottom parameter values to be found in Table 1. For all exact scenarios we will have true $z_{ph1} = 14.6\text{m}$ and true ranges $r_{ge} = 265, 480, 780, 980,$ and 2075m .

	thin	medium	thick
h_{sed}	12m	22m	40m
c_{sed}	1622m/s	1644m/s	1610m/s
γ	2.0/s	-4.0/s	0
c_{hsp}	1806m/s	1856m/s	1900m/s
z_{sou}	29.4m	31.4m	31.2m
D	78.2m	79.7m	80.8m

Table 1: Table of geometric and environmental values for the three sediment thicknesses (simulated) considered. h_{sed} is the sediment thickness, c_{sed} is the sound-speed at the top of the sediment, γ is the sound-speed gradient in the sediment (sound-speed at the bottom of the sediment is given by $c_{sed} + \gamma h_{sed}$), c_{hsp} is the sound-speed of the basement half-space, z_{sou} is the source depth, and D is the water depth.

Unfortunately, this summation approach does *not* indicate when component frequencies have contributed low levels. Moreover, the summation MFP level can remain high even when a small subset of components values is legitimately very low. Thus, the summation method can smear out MFP levels so that sensitivity is actually reduced (the curve is less peaked with slower sidelobe level degradation) making it harder to find “true” parameter values. Thus, one can trade “robustness” for “sensitivity”. See Tolstoy, ’12b, for greater detail on the method.

Consider the “thin” sediment case. In Fig. 2 we see the linear MFP behavior as a function of c_{hsp} for a few frequencies (as indicated: 25, 50, 75, and 100Hz) and at $rge = 980m$. We assume here that all parameters other than c_{hsp} are known exactly. First, we note that there are sidelobe differences per frequency (as expected). Next, we note that there are sensitivity differences with maximum sensitivity at 25Hz. Finally, we note that although the behavior varies as a function of frequency, it is impossible to predict the specific behavior as it does not vary systematically. For our example, frequency 100Hz shows more sensitivity than 50Hz while 75Hz is more sensitive than 100Hz.

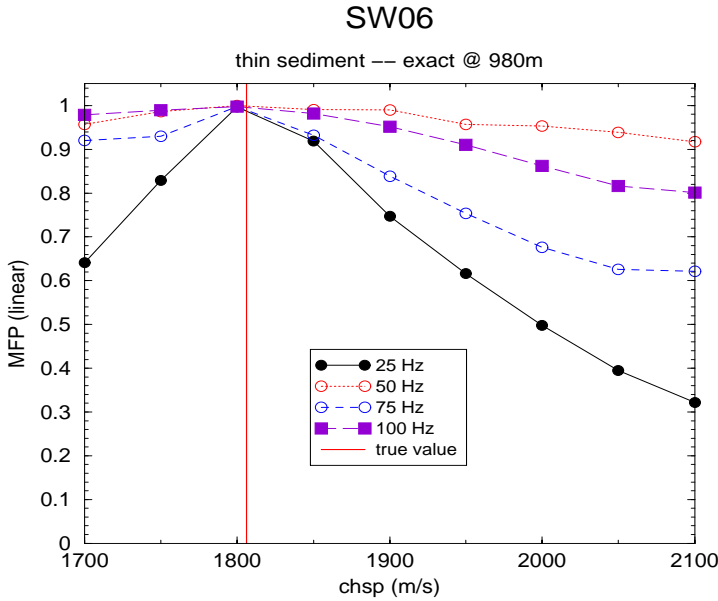


Figure 2: Multi-frequency linear processor results at a thin sediment for c_{hsp} at $rge = 980m$.

Consider a broadband average (over 16 frequencies 25 to 100Hz, $\Delta f = 5\text{Hz}$). In Fig. 3a we see that the average $\mathcal{P}_{lin,ave}(\mathbf{p})$ (the solid line with the filled in black circles) has improved the sensitivity and reduced sidelobes compared to some but not all f , e.g., compared to 50Hz but not compared to 25 or 75Hz (as seen in Fig. 2). If we consider $\mathcal{P}_{min}(\mathbf{p})$ as shown by the dashed line with the open circles (and in this example the curve actually corresponds to that seen in Fig. 2 for 25Hz), then we now have significantly more sensitivity than for the straight average. That is, we see significant sidelobe reduction for the new processor. Thus, for this parameter c_{hsp} we have been able to improve sensitivity relative to the averaging processor, and the new processor is dominated automatically by the low frequency 25Hz component. Consider another parameter: h_{sed} .

In Fig. 3b we see the behavior of $\mathcal{P}_{lin,ave}(\mathbf{p})$ versus $\mathcal{P}_{min}(\mathbf{p})$ for the more problematic parameter h_{sed} where \mathbf{p} varies from (1806,5,1622,2) to (1806,55,1622,2) in 1m increments for h_{sed} . This parameter often has a number of local maxima (as seen here) thereby complicating convergence for inversion methods. First, we again see that while the averaged linear method shows some sensitivity to this parameter, this sensitivity is significantly increased for the minimization method. That is, sidelobes overall have been reduced much more efficiently for \mathcal{P}_{min} . Second, for this parameter h_{sed} the new processor has been dominated by the 85-90Hz components (not shown individually and we recall that here $c(z)$ is known exactly). That is, we again have that the new processor is dominated automatically by certain frequencies.

In Fig. 3c we see the behavior of c_{sed} where the higher frequencies contribute the best resolution (80Hz and above where we still have $c(z)$ known exactly). In general, it seems that c_{sed} has the best sensitivity at the highest frequencies. Unfortunately, those higher frequencies are most susceptible to experimental errors. We again notice that (as for the other parameters) the minimization processor shows the better sidelobe reduction for our unknown parameters, and it is dominated automatically by certain frequencies.

These conclusions still hold true at longer ranges, and for other component processors (such as the minimum variance rather than the linear). That is, sensitivity is improved with the new processor with automatic emphasis on the most sensitive f . Clearly, the new processor shows promise relative to the averaged BB linear processor – when things are known perfectly. However, one of the strong points for the averaging MFP is that when things are *not* known exactly, i.e., when there are errors in our assumptions (as in a test situation), the usual approach is known to be quite stable and not overly disturbed by an occasional frequency misstep. What happens for \mathcal{P}_{min} ?

In particular, let us assume that:

- $\gamma = 0$ (thus we will be inverting for the approximate c_{ave} in the sediment layer;
- source range rge is known only to within 100m (rge and water depth D are known to be linearly related – even broadband processing cannot separate out the “true” values of rge and D ; see Tolstoy et al., '12a). Thus, we will invert only for D assuming a “known”, i.e., approximate, rge;
- the ocean sound-speed $c(z)$ will be assumed by the dashed (incorrect) curve of Fig. 1;
- z_{sou} will be fixed at 30m (rather than its “true” value which will vary as in Table 1);

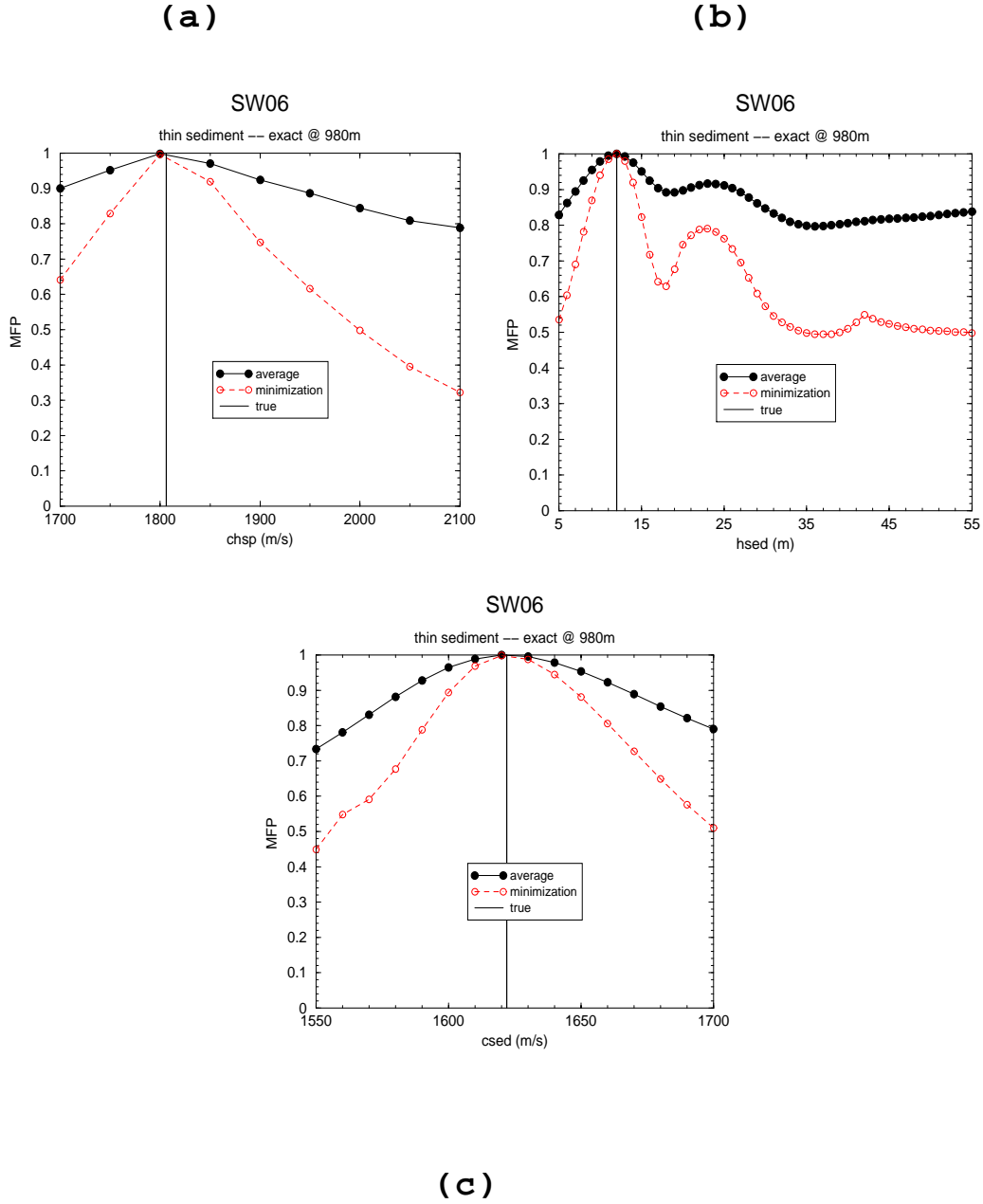


Figure 3: $\mathcal{P}_{ave,lin}$ and \mathcal{P}_{min} (linear MFP components) for 16 frequencies 25 to 100Hz at 5 Hz increments, with $\mathbf{rge} = 980m$, assuming the thin sediment scenario and other parameters known exactly. (a) The parameter considered is c_{hsp} varying from 1700m/s to 2100m/s. The true value is 1806m/s. (b) The parameter considered is h_{sed} varying from 5m to 55m. The true value is 12m. (c) The parameter considered is c_{sed} varying from 1550m/s to 1700m/s. The true value is 1622m/s.

- for the VLA we will assume top phone depth at $z_{ph1} = 15.6\text{m}$ (a shift error of 1m depth for all phones).

In Fig. 4a (comparable to Fig. 3a but at $rge = 2075\text{m}$ plus our errors) we see that $\mathcal{P}_{min}(\mathbf{p})$ has degraded a lot with lower peaks of 0.71 at $\mathbf{p} = (1800, 12, 1630, 0)$, 0.77 at $\mathbf{p} = (1800, 11, 1630, 0)$, and 0.74 at $\mathbf{p} = (1800, 12, 1640, 0)$. We also observe that non-peak values have again decreased much more than $\mathcal{P}_{ave,lin}(\mathbf{p})$, and that the new peaks can be in different erroneous locations (not equivalent to simply raising the linear processor to some power). Thus, even in the presence of our errors $\mathcal{P}_{min}(\mathbf{p})$ shows very good sidelobe reduction. But what about those rather low (and incorrectly shifted) peak values? These low values (less than 0.9) turn out to occur consistently at frequencies above 60 Hz. Such higher frequency values are understandably more affected by our errors. However, if we restrict our new processor to f 25-60 Hz, then we get the results seen in Fig. 4 for the starred curves, i.e., great performance with correct, strong peaks and much reduced sidelobes.

Why do we care about this proposed method? First, the method offers improved efficiency in sequential inversion computations. In particular, let us begin the inversions at a parameter point \mathbf{p} at a low frequency (sequential with frequency) and then increase frequency in steps. If at any step we find that $\mathcal{P}_{lin}(f, \mathbf{p})$ is less than our target amount (a fairly high value set by the user), then we can cease the frequency computations and move to another parameter point. Thus, many points may be quickly eliminated.

Additionally, at LFs we can employ cruder sampling of the multi-dimensional solution space. Restricting the processor to rather low frequencies such as 25-60Hz can mean that fewer parameters at cruder sampling intervals will need to be considered to find all the peaks.

This method also indicates when frequency difficulties appear. That is, consistently low MFP values suggest a problem. Then, the user can study why and when such persistent low MFP values occur. Is the signal-to-noise level low? Is there an erroneous assumption somewhere? In general, such results can act as a helpful source of debugging as well as of general information about the inversion itself.

Next, this new method can be insensitive to expected errors in parameters assumed to be “fixed” such as z_{ph_i} . The technique allows for more error in the experimental measurements.

Finally, this method also offers improved parameter resolution. In particular, it automatically emphasizes those frequencies which are sensitive to our parameters of interest. That is, it does not smear out that sensitivity over a wide range of frequencies (as happens with general incoherent summation) but rather is dominated by the sensitivity offered by *any* frequency component.

What are potential problems? This approach will not work if there are low signal-to-noise levels at any of the final component frequencies. A requirement for this method is that each frequency contribution not be “too” erroneous. A band of frequencies, e.g., above 60Hz, may be eliminated *if* their contributions *are* problematic – so long as those difficulties are understood (severely affected by expected experimental errors or false assumptions about the environment?).

Thus, we conclude from this year’s work that the new minimization method:

- is broadband;

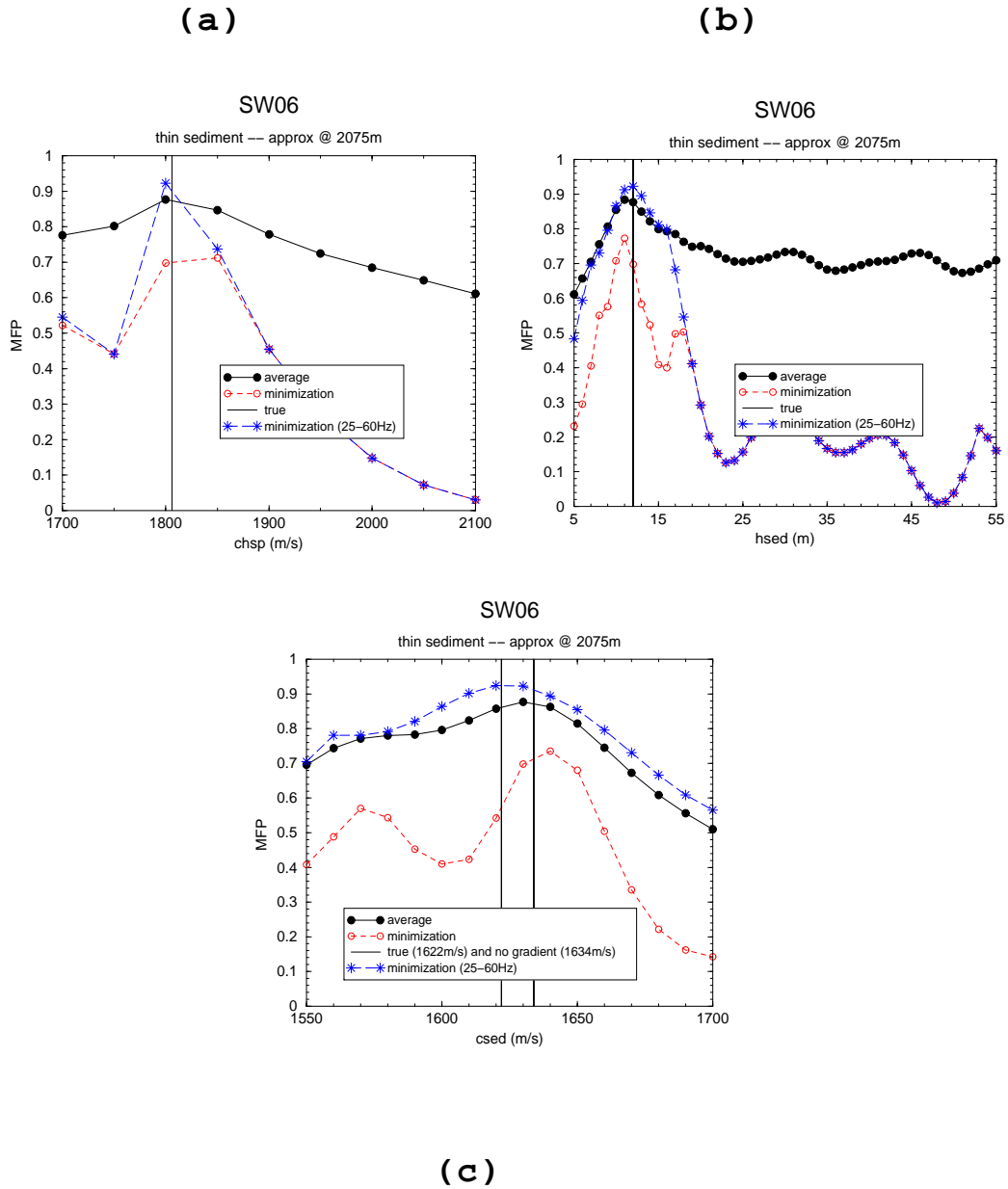


Figure 4: Same as Fig. 3 except that small errors have been assumed (environmental parameters are known only approximately) and we are at $rge = 2075m$. We also have curves (starred, dashed) for \mathcal{P}_{min} computed using only frequencies 25-60Hz (we recall that the low peak values ended up indicating errors in the higher frequencies). (a) c_{hsp} , (b) h_{sed} , and (c) c_{sed} .

- will be dominated automatically by those frequencies which are most sensitive to unknown parameters;
- improves sensitivity and resolution compared to incoherent broadband summation (for any component processor such as the linear or minimum variance processor);
- can improve inversion efficiency (for sequential f computations);
- shows sidelobe improvement even in the presence of (our expected) errors;
- indicates when something is wrong, i.e., the peak value will be “low”. Such problems need to be pursued to understand why that has happened. The method can also indicate when a band of component frequencies has a problem, and this can lead to the adoption of only the low frequency components.

As a final note, implementation of the new method should be easy – it can simply replace the incoherent summation of components with a minimization function.

WORK COMPLETED

Recent work (FY08) completed includes:

- continued development of a new BB signal processing method ($\mathcal{P}_{min}(f)$);
- application of the minimization method to several simulated SW06 scenarios (single sediment layer: thin, medium, or thick);
- extension to longer ranges (incorporation of KRAKEN for more speed assuming range-independence) in anticipation of application to Knobles data;
- examination of the minimization method sensitivity as a function expected errors (in ocean sound-speed $c(z)$, source depth z_{sou} , and in VLA depth z_{phi}).

RESULTS

We have a new BB processor $\mathcal{P}_{min}(f)$ which promises excellent resolution for G.I. at LFs (f within 25-75Hz) and at close ranges (within 250m to about 1km), and even in the presence of expected test errors. This processor will also indicate when it has trouble (it will show low MFP values).

IMPACT/APPLICATION

As a result of the work this past year we have developed and better understand:

- the LF G.I. method as applied to a variety of simulated SW06 data, particularly with regard to sensitivity for bottom parameters as a function of frequency and range;
- the effects of expected errors in a SW06 test environment;
- a new BB inversion method (relative to standard BB incoherent averaging) with demonstrated success on simulated SW06 data;

- the potential success of HLAs for G.I.

RELATED PROJECTS

The G.I. work is related to work by R. Chapman and colleagues (U. Victoria), D. Knobles and colleagues (U. Texas at Austin), W. Hodgkiss and colleagues (Scripps), and other researchers in SW06 and shallow water inversion (such as P. Gerstoft, P. Nielsen, C. Harrison).

REFERENCES

- Collins, M.D. (1994), “Generalization of the split-step Pade solution”, *J. Acoust. Soc. Am.* **96**, 382-385.
- Gerstoft, P., Hodgkiss, W.S., Kuperman, W.A., and Song, H., “Phenomenological and global optimization inversion”, *J. Ocean. Eng.* **28**(3), 342-354 (2003).
- Jiang, Y.M. and Chapman, N.R. 2009, “The impact of ocean sound-speed variability on the uncertainty of geoacoustic parameter estimates”, *J. Acoust. Soc. Am.* **125** (5), 2881-2895.
- Tolstoy, A., Jesus, S., and Rodriguez, O. 2002, “Tidal effects on MFP via the Intimate96 data” in *Impact of Littoral Environmental Variability of Acoustic Predictions and Sonar Performance* ed. Pace & Jensen, Kluwer Academic Pubs, 457-463.
- Tolstoy, A. (1993), *Matched Field Processing in Underwater Acoustics*, World Scientific Publishing, Singapore.
- Tolstoy, A. (2010), “A deterministic (non-stochastic) low frequency method for geoacoustic inversion”, *J. Acoustic. Soc. Am.* **127**(6), 3422-3429.
- Tolstoy, A. (2012a), “Bottom parameter behavior in shallow water”, *J. Acoust. Soc. Am.*, **131**(2), 1701-1710 (2012).
- Tolstoy, A. (2012b), “An improved broadband matched field processor for geoacoustic inversion”, to appear as a Letter in *J. Acoust. Soc. Am.*, Oct. 2012.

PUBLICATIONS for FY10 - FY12 (this contract period)

- Tolstoy, A. (2012b), “An improved broadband matched field processor for geoacoustic inversion”, to appear as a Letter in *J. Acoust. Soc. Am.*, Oct. 2012.
- Tolstoy, A. (2012a), “Bottom parameter behavior in shallow water”, in a special issue of *J. Acoust. Soc. Am.* **131**(2), 1701-1710.
- Tolstoy, A. (2011), “A new broadband matched field processor?”, abstract for talk presented at ASA meeting (San Diego CA Nov).
- Tolstoy, A. (2011), “Broadband geoacoustic inversion on a horizontal line array”, abstract for talk presented at ASA meeting (San Diego CA Nov).

- Tolstoy, A. (2010), “A deterministic (non-stochastic) low frequency method for geoacoustic inversion”, *J. Acoustic. Soc. Am.* **127**(6), 3422-3429.
- Tolstoy, A. (2010), “Waveguide monitoring (such as sewer pipes or ocean zones) via matched field processing”, *J. Acoustic. Soc. Am.* **128**(1), 190-194.
- Tolstoy, A. (2010), “Using low frequencies for geoacoustic inversion”, in *Theoretical and Computational Acoustics 2009*, Dresden, ed. S. Marburg.
- Tolstoy, A. (2010), “Geoacoustic Inversion Algorithms when do we stop?”, abstract for talk presented in Cambridge UK April 7-9 2010.
- Tolstoy, A. (2010), “The estimation of geoacoustic parameters via frequencies 25 to 100Hz” abstract for talk presented at ASA meeting (Baltimore MD Apr).
- Tolstoy, A. and M. Jiang (2009), “The estimation of geoacoustic parameters via low frequencies (50 to 75Hz) for simulated SW06 scenarios”, abstract for talk presented ASA meeting (Austin TX Oct).

HONORS/AWARDS

- Associate editor for JASA (2004-2012)
- Associate editor for JCA
- member of ASA Committee on Underwater Acoustics
- member of ASA Committee on Acoustical Oceanography